

Supplementary Information

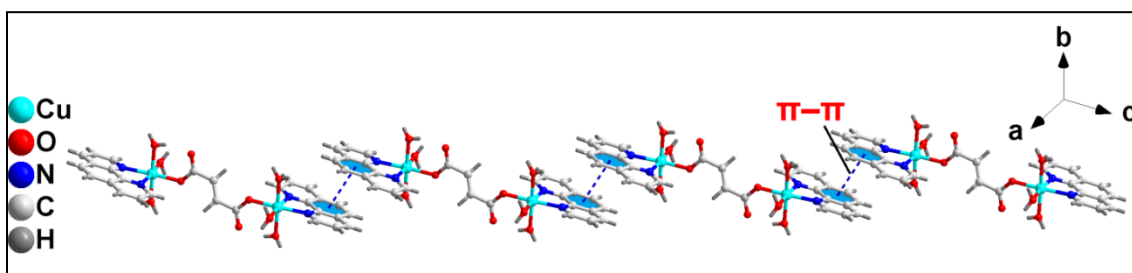


Fig. S1 1D supramolecular chain of compound 1 assisted by π -stacking interactions.

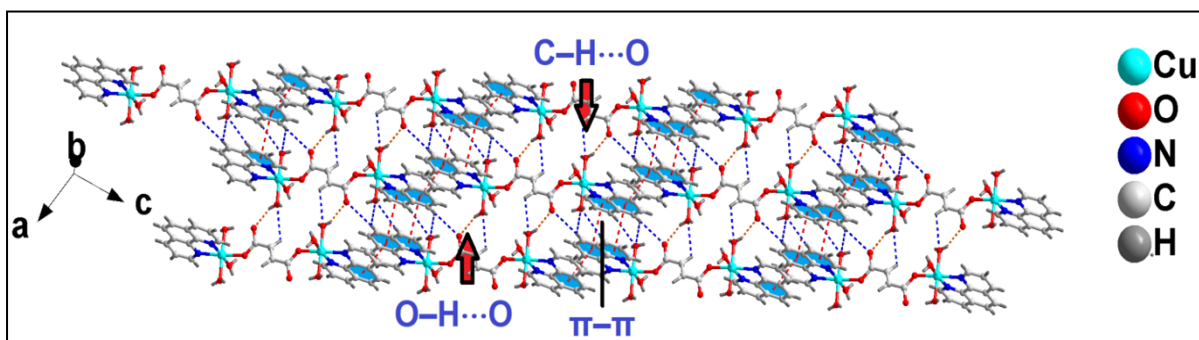


Fig. S2 Layered architecture of compound 1 assisted by cooperative $(\pi-\pi)_2/(\pi-\pi)_1/(\pi-\pi)_2$ ternary assemblies, O-H...O and C-H...O hydrogen bonding interactions.

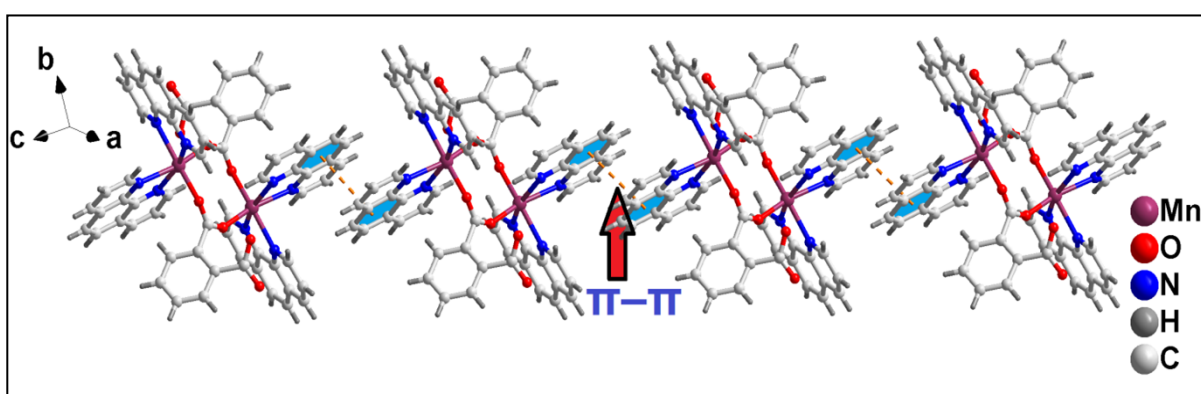


Fig. S3 1D supramolecular chain of compound 2 assisted by π -stacking interactions.

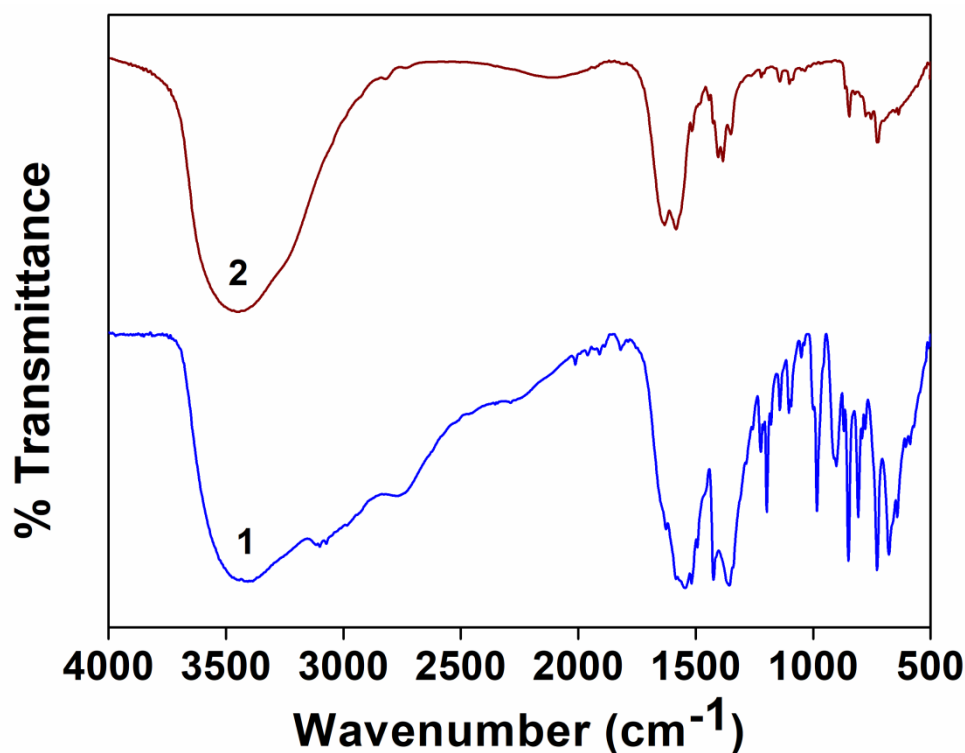


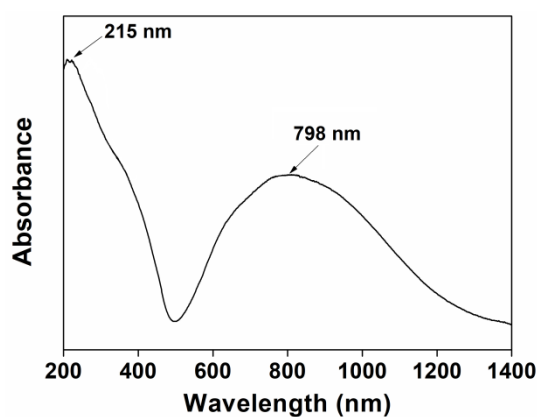
Fig. S4 FT-IR Spectra of compounds **1** and **2**.

3.4 Electronic spectroscopy

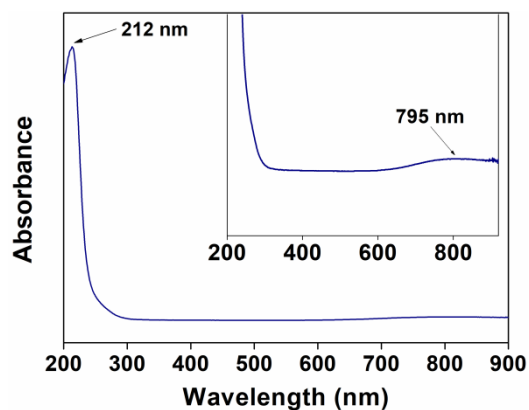
The electronic spectra of the compounds have been recorded in both solid and in solution phases in PBS (5% DMSO) (Figs. S5 and S6). The solid state UV-Vis-NIR spectrum of **1** (Fig. S5a) exhibits peaks at 215 nm assigned to $\pi \rightarrow \pi^*$ transitions of the aromatic ligand.¹ The spectrum (Fig. S5a) shows broad absorption band at 798 nm resulting from the usual ${}^2E_g \rightarrow {}^2T_{2g}$ transition for Cu(II) complexes.² In the UV-Vis spectra (Figs. S5b-S5e) of the compounds, the absorption peaks for $n \rightarrow \pi^*$ and ${}^2E_g \rightarrow {}^2T_{2g}$ transitions are obtained at the expected positions.²

The spectra of compound **2** show no absorption bands in the visible region, as the Mn(II) centre (d^5 system) has all the electronic transitions from the ${}^6A_{1g}$ ground state are doubly forbidden.³ The peaks for $\pi \rightarrow \pi^*$ absorption of the *phen* are obtained at the expected positions (Fig. S6).⁴

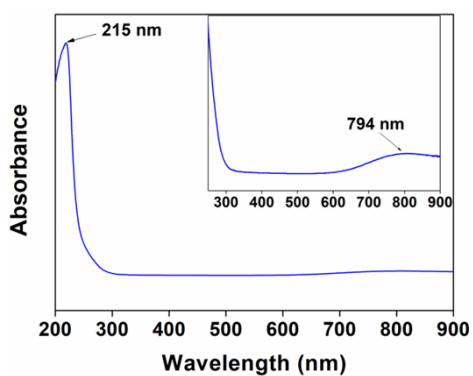
The similar absorption bands observed in the solid and solution phase electronic spectra of the compounds indicate that the compounds do not undergo any structural distortion in the aqueous phase.⁵



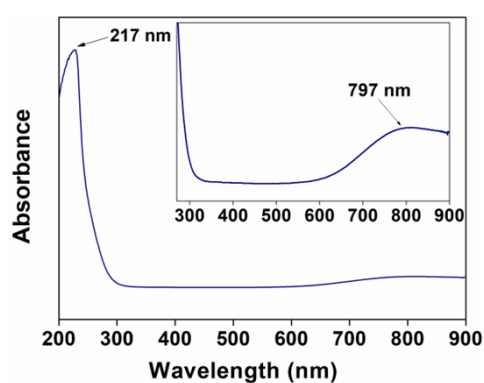
(a)



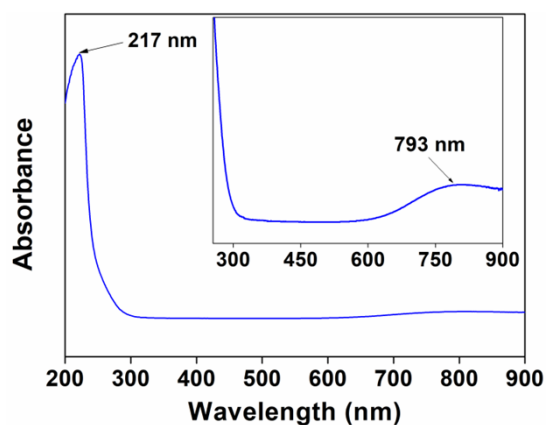
(b)



(c)

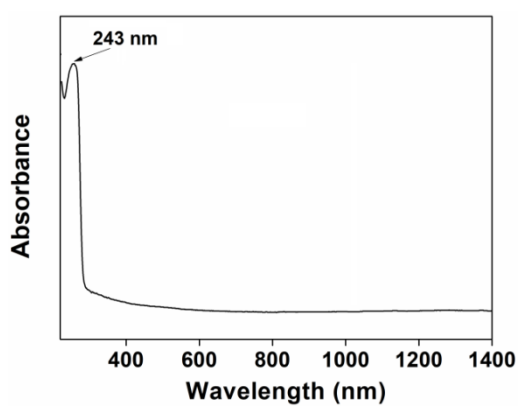


(d)

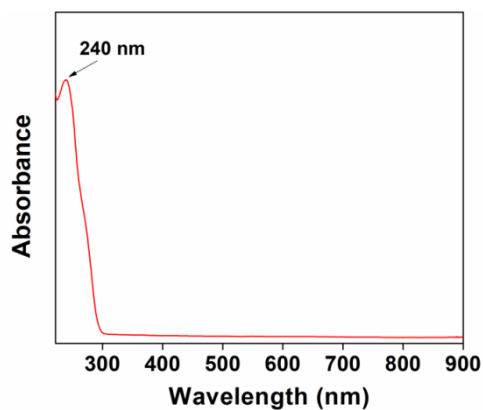


(e)

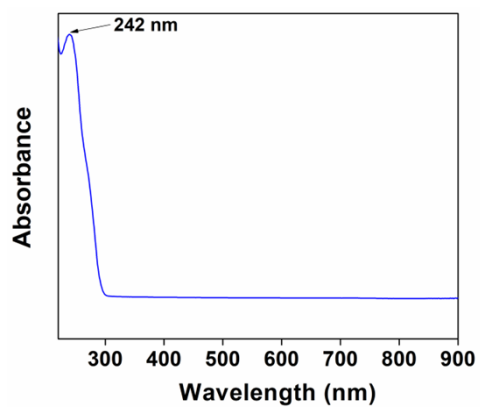
Fig. S5(a) UV-Vis-NIR spectrum of compound **1**; **(b)** UV-Vis spectrum of **1** (0 hour); **(c)** UV-Vis spectrum of compound **1** (6 hours); **(d)** UV-Vis spectrum of compound **1** (12 hours); **(e)** UV-Vis spectrum of compound **1** (24 hours). The spectra of the compounds were recorded in PBS (5% DMSO) medium.



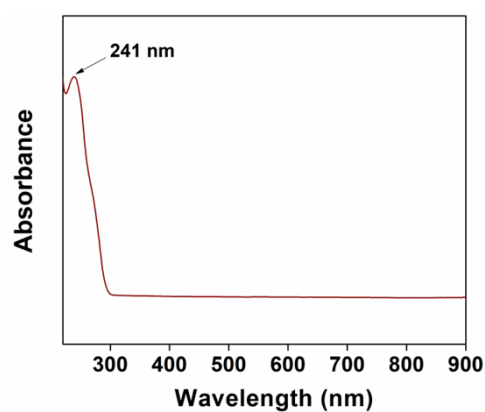
(a)



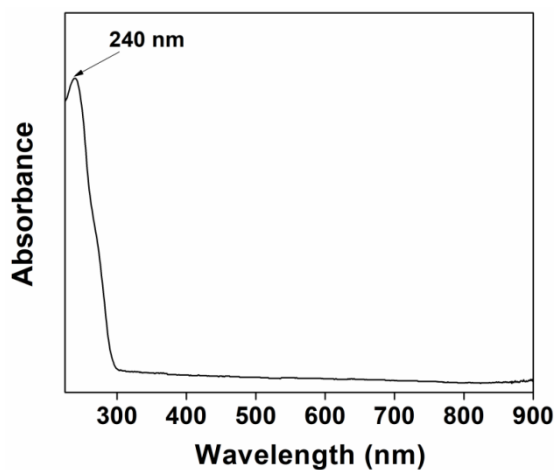
(b)



(c)



(d)



(e)

Fig. S6(a) UV-Vis-NIR spectrum of compound **2**; **(b)** UV-Vis spectrum of **2** (0 hour); **(c)** UV-Vis spectrum of compound **2** (6 hours); **(d)** UV-Vis spectrum of compound **2** (12 hours); **(e)** UV-Vis spectrum of compound **2** (24 hours). The spectra of the compounds were recorded in PBS (5% DMSO) medium.

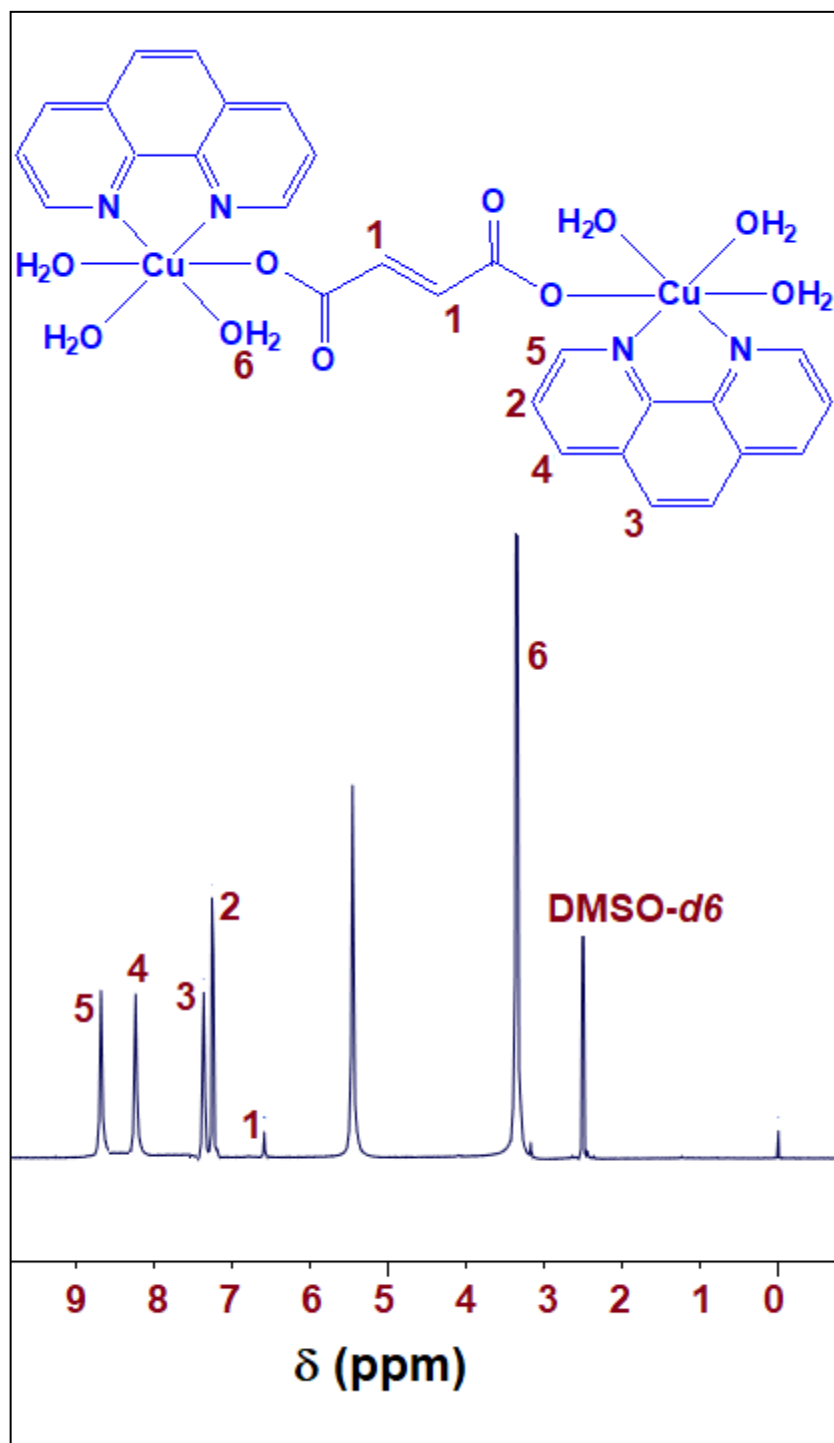


Fig. S7 ¹H-NMR spectrum of compound 1 in DMSO-*d*₆.

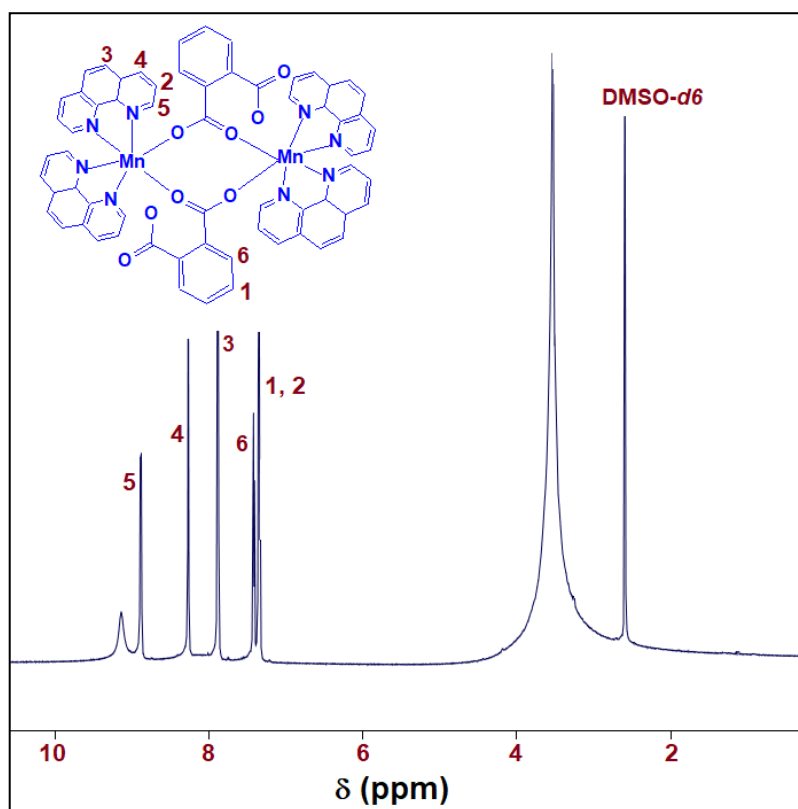


Fig. S8 $^1\text{H-NMR}$ spectrum of compound **2** in $\text{DMSO-}d_6$.

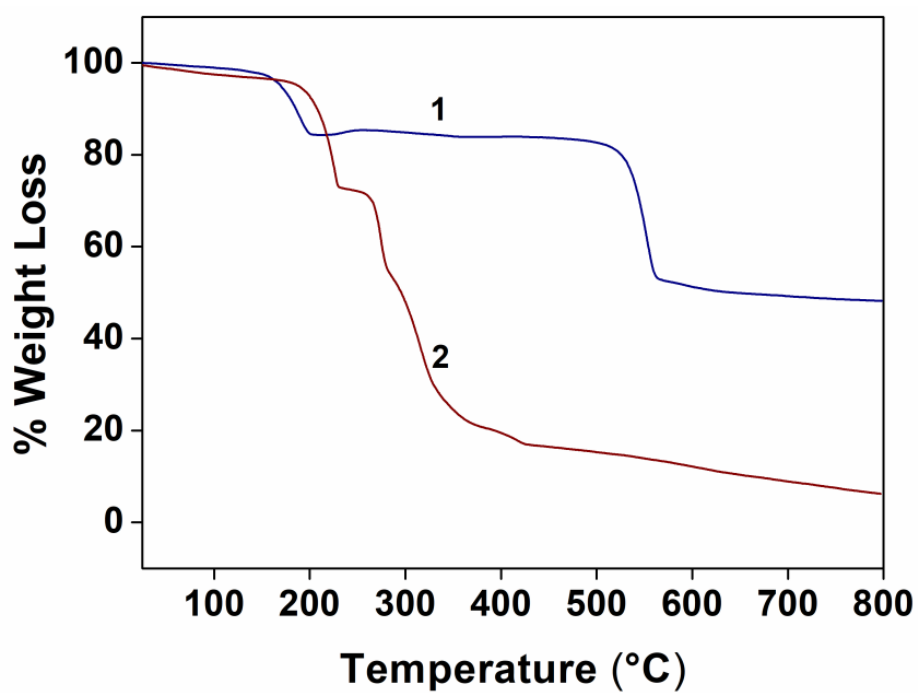


Fig. S9 Thermogravimetric curves of the compounds **1** and **2**.

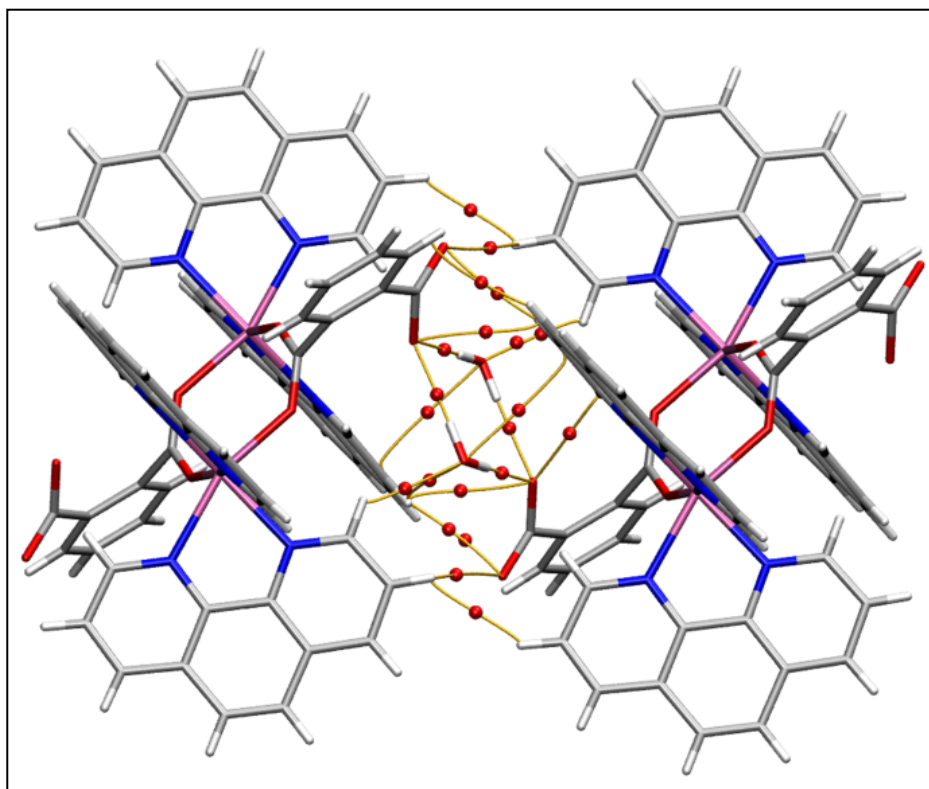


Fig. S10 Combined QTAIM (bond CPs in red and bond paths as orange lines) and NCI plot ($|R_{GD}| = 0.55$, density cut-off = 0.04 a.u., colour range $-0.04 \text{ a.u.} \leq (\text{sign}\lambda_2)\rho \leq 0.04 \text{ a.u.}$) for the tetrameric assembly of compound **2**. The H-bond energies estimated using the potential energy density (V_r) are indicated in red.

Table S1 Intermolecular interactions are shown between receptors (BCL-2 and BCL-XL) and compound **1** along with respective reference ligands (associated with PDB structure file). As per binding energy algorithm, lowest the score better is the binding affinity.

Receptors	Ligands	Docking score	H- bond score	Interacting residues
BCL-2 (PDB:2O22)	Reference ligand	-165.21	-6.81	Tyr105, Gly142, Tyr199, Phe101, Val145, Phe109, Ala146
	Compound 1	-153.41	-3.10	Arg104, Ala97, Tyr199, Val145
BCL-XL (PDB:2YXJ)	Reference ligand	-152.22	-7.66	Glu96, Val141, Gly138, Tyr195, Arg139, Tyr101, Leu130, Ala104, Phe97, Ala142, Leu108, Phe105
	Compound 1	-122.18	-2.82	Ala104, Glu129, Leu130, Gly138, Ala142, Leu108

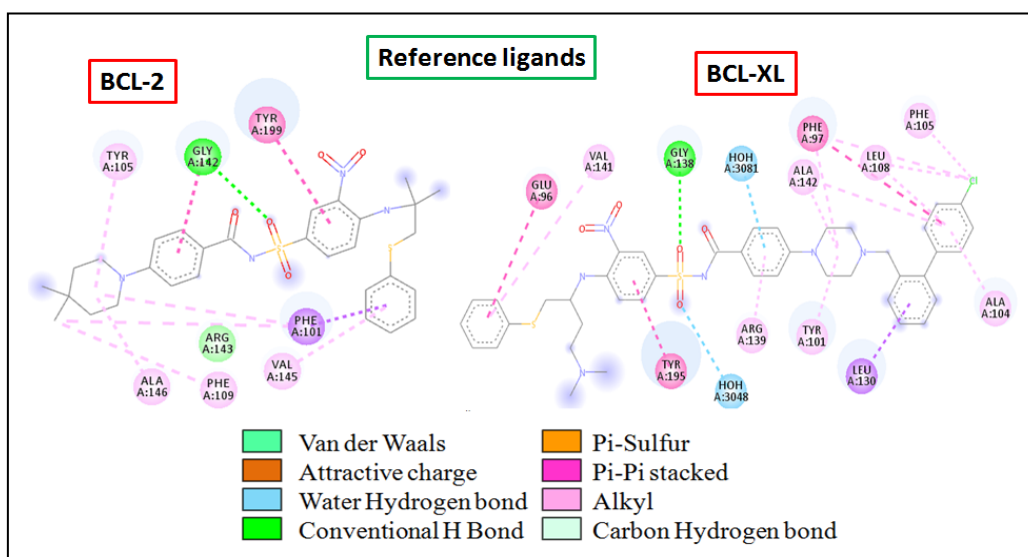


Fig. S11 Docking structures of reference ligands with BCL-2 (PDB: 2O22) and BCL-XL (PDB: 2YXJ) receptors are shown. Chemical interactions are shown along with ligand atoms and interacting amino acids in the inhibitors binding sites of both receptors. The detailed information about the reference ligands can be obtained from the given PDB file code.

Supplementary References

- 1 C. Singh, S. Mukhopadhyay and S. K. Das, *Inorg. Chem.*, 2018, **57**, 6479-6490.
- 2 (a) S. Choubey, S. Roy, K. Bhar, R. Ghosh, P. Mitra, C. Lin, J. Ribas and B. K. Ghosh, *Polyhedron*, 2013, **55**, 1-9;
 (b) L. K. Das, S. W. Park, S. J. Cho and A. Ghosh, *Dalton Trans.*, 2012, **41**, 11009-11017.
- 3 (a) A. Majumder, C. R. Choudhury, S. Mitra, C. Marschner and J. Baumgartner, *Z. Naturforsch.*, 2005, **60b**, 99-105;
 (b) O. Horner, J. Girerd, C. Philouze and L. Tchertanov, *Inorg. Chim. Acta*, 1999, **290**, 139-144.
- 4 O. V. Sizova, A. Y. Ershov, N. V. Ivanova, A. D. Shashko and A. V. Kuteikina-Teplyakova, *Russ. J. Coord. Chem.*, 2003, **29**, 494-500.
- 5 (a) H. Nath, D. Dutta, P. Sharma, A. Frontera, A. K. Verma, M. Barceló-Oliver, M. Devi and M. K. Bhattacharyya, *Dalton Trans.*, 2020, **49**, 9863-9881;
 (b) C. Yenikaya, M. Poyraz, M. Sari, F. Demirci, H. Ilkimen and O. Buyukgungor, *Polyhedron*, 2009, **28**, 3526-3532.